Improvement of the hempcrete-phase change material wall performance during the heating season using temperature control strategies

Yaser Abdellatef[1,2], Miroslava Kavgic[1]

[1]Civil Engineering, University of Ottawa, 161 Louis Pasteur, Ottawa, Ontario, Canada, K1N 6N5

[2]Mechanical Power Department, Faculty of Engineering, Cairo University, 12613 Giza, Egypt

Abstract

Phase change material (PCM) enhanced wall assemblies can control indoor temperatures and save energy. However, PCM needs to change the phase to be fully effective. The integration of PCMs into building envelopes typically requires mixing with other materials. This research aims to advance the existing knowledge on incorporating PCM into carbon-neutral wall assemblies made of hempcrete and investigating temperature control strategies to improve wall systems' performance during the heating season. A 30 cm hempcrete and hempcrete-PCM walls were simulated in Fluent under Ottawa weather conditions and compared under different temperature control strategies. Overall the hempcrete-PCM (HPCM) enhanced wall outperformed the hempcrete wall during the heating season.

Keywords: Phase change materials, Hysteresis, Hempcrete, Passive application, Temperature controls

Introduction

The building sector consumes around 40 % of global energy demand and produces nearly 30% of energy-related carbon dioxide emissions (Pérez-Lombard et al., 2008). As a result, it is one of the main contributors to global warming and greenhouse gas emissions. Innovative energy-saving technologies such as phase change materials (PCMs) could reduce energy consumption while improving thermal comfort (Al-Janabi and Kavgic, 2019).

PCMs are a latent heat storage technology that can absorb and release large amounts of energy per unit mass through the phase change process from liquid to solid and back (Zhou et al., 2012). Hence, PCM integration in buildings can control indoor temperatures and result in considerable energy savings by absorbing energy during the daytime through melting (charging cycle) and releasing this energy back during the colder nighttime through returning to its solid-state (discharging cycle). Moreover, PCM can be passively integrated into the building materials without the need for auxiliary equipment (Zhou et al., 2012) via different techniques such as PCM-enhanced covering materials, including plasterboards, wallboards or gypsum boards (Wijesuriya et al., 2018), concrete (Ren et al., 2021), ceramics (Krasoń et al., 2019), micro-encapsulated PCM panels (Rathore and Shukla, 2019), PCM-impregnated insulations (Torres-Rodríguez et al., 2020), and micro-encapsulation (Abdellatef and Kavgic, 2020, Abdellatef et al., 2022).

Construction materials' sustainability and energy intensity are becoming more critical by tightening the building energy codes with decreasing operational loads. Most previous research used high embodied energy construction materials, such as gypsum (Toppi and Mazzarella, 2013), concrete (Lecompte et al., 2015), and cement mortars (Franquet et al., 2014), for mixing with PCMs. Hempcrete, made of the hemp plant's inner woody core mixed with a lime-based binder, is a carbon-negative, lightweight, biocomposite material that can significantly enhance energy performance, indoor environmental quality, and sustainability of buildings (Stanwix and Sparrow, 2014, Pochwala et al., 2020). In this regard, hempcrete has low thermal conductivity in the range of 0.06-0.14 W/m K (Evrard and Herde, 2005, Evrard, 2008, Yates, 2002) and a high specific heat capacity from 1000 to 1590 J/kg K, resulting in low thermal diffusivity ranging from 1.48×10^{-7} m^2/s in the dry state to 0.98×10^{-7} m^2/s in the fully saturated condition (Walker and Pavía, 2014, Abdellatef et al., 2020). Additionally, hempcrete can be integrated with PCM to improve its thermophysical properties leading to higher energy savings than hempcrete (Kavgic and Abdellatef, 2021, Abdellatef and Kavgic, 2020).

Moreover, PCM should undergo a phase change from solid to liquid and vice versa to become fully operative. Hence, an appropriate control strategy with a proper amount of PCM is required to achieve suitable conditions for the phase transition and maximize the energy savings during its operation. Different control techniques have been tested in buildings with PCM-integrated envelopes to achieve indoor comfort and minimize energy consumption, cost, and CO_2 emissions (Gholamibozanjani and Farid, 2021). Thus, (Solgi et al., 2017) implemented night ventilation that caused PCM solidification when the outdoor temperature

went below 30 °C to decrease the cooling energy of an office building subjected to a hot-arid climate. In addition, (Zhu et al., 2011) performed numerical research to investigate the effect of optimal control techniques in commercial buildings integrated with shape stabilized PCM and air conditioning units. The results showed that using PCM in the building envelope caused a reduction in electricity and peak load by 11% and 20%, respectively.

Nevertheless, limited research studied the influence of indoor schedules and temperature control strategies on the performance of thermal mass envelope systems. For instance, (Bastani et al., 2015) examined the effect of an on/off control strategy on shifting heating peak demand for a bungalow built with PCM wallboards in Canada, using five setpoint temperatures (20–25, 19–24, 18–23, 20–24, and 20–23 °C). During the charging period and the entire day, a broader range of room temperatures results in greater energy consumption. At the same time, a wider range of temperature allowed the heater to remain operational for a more extended period after the charging hours. Another study (Hagenau and Jradi, 2020) examined seventeen PCMs in a standard Danish office using a cooling setpoint of 25 °C and a heating setpoint of 22 °C. The setpoint temperature ranged between 21–23 °C during off-peak hours and 17–19 °C during peak hours. A PCM-enhanced hut saved 21.5% in power and 26.7% in costs over six days compared to a structure without PCM. The results suggest that building insulation, room cooling, heating setpoints, and weather conditions were essential in determining the best-performing PCM. Furthermore, (Abdellatef and Kavgic, 2020) reported that hempcrete-PCM composites achieved approximately 5-16% and 1-36% higher heating and cooling energy savings than hempcrete, respectively, owing to their lower thermal conductivity and higher specific heat capacity. However, they also reported approximately 2-14% reductions in heating and cooling energy savings due to increased PCM's percentage share from 9% to 18% and emphasized the need for changes in heating and cooling systems' operation to improve the performance of PCM-enhanced envelope systems.

Moreover, (Kavgic and Abdellatef, 2021) investigated different control techniques to enhance the performance of hempcrete and hempcrete-PCM enhanced walls exposed to the extreme weather conditions of Winnipeg, which belongs to climate zone 7A and is the second sunniest city in Canada. They concluded that during days with high solar radiation, phase change material melted and absorbed heat, thus increasing the energy use compared to the hempcrete wall. Therefore, the optimal applications of thermal energy storage materials in building envelopes require their integration with HVAC systems and temperature controls that facilitate the charging and discharging of these thermal batteries.

This study aims to further the current research on hempcrete-PCM composites integration into wall assembly systems and apply different temperature control strategies to improve their performance in milder cold climate zone 6 with 4000–4999 heating degree days (HDD) but with lower solar radiation than climate zone 7A (5000 – 5999 HDD) of Winnipeg. ANSYS Fluent was used to model the wall assembly while allowing the hysteresis effect and control strategy simulation through the user-defined functions. First, hempcrete and hempcrete-PCM (HPCM) wall configurations were modeled using thermophysical experimental properties (Abdellatef and Kavgic, 2020). Second, we analysed and compared the walls' performance under the base-case control strategy. We then investigated their performance under four different control strategies designed to decrease heating and cooling energy consumption while improving the phase change transition of the microencapsulated PCM. This research furthers our knowledge and understanding of the behaviour of latent heat storage walls in cold climates under various temperature control strategies. Thus, it provides valuable recommendations for the integrated building design that considers the interaction between the building envelope HVAC systems.

Materials & Methods

Through numerical simulations, the experimental results (Abdellatef and Kavgic, 2020) have been extended to compare the performance of hempcrete and HPCM wall structures under different control approaches. Figure 1 shows the wall with 30 cm of (hempcrete / HPCM) infill model developed in ANSYS.

A hempcrete infill comprises hemp hurd, binder (50% hydrated lime and 50% metakaolin by weight), and water at a ratio of 1:1:3 by weight, respectively. HPCM infill consists of approximately 9% microencapsulated phase change material (MPCM) (Nextek 18D) and 91% hempcrete because of MPCM's high price, adverse effects on mechanical properties (Navarro et al., 2016), and hindering impact on energy savings when used in higher percentages (Abdellatef and Kavgic, 2020). The Nextek 18D product has an 18±1 °C phase change temperature and ≥190 J/g heat of fusion. We selected Nextek 18D because of its high shell integrity, volumetric heat capacity, low agglomeration rate, and high encapsulation efficiency (Abdellatef and Kavgic, 2020). The hempcrete and HPCM infills values are based on the experimental study (Abdellatef and Kavgic, 2020). Common building materials, including gypsum and cement lime plaster, are obtained from the WUFI software library. Table 1 provides the materials' thermophysical properties.

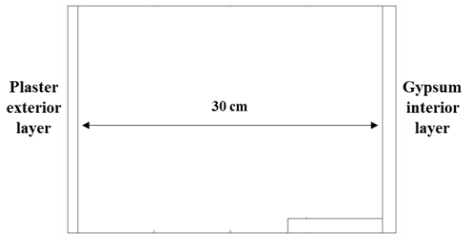

Figure 1. Wall geometry and design configurations.

Table 1. Thickness and thermophysical properties of the simulated materials.

Material	Gypsum	Cement lime plaster	Hempcrete	HPCM
Thickness (cm)	2	1.5	30	30
Density (kg/m^3)	675	1900	316	327
Conductivity (W/m K)	0.202	0.803	0.103	0.093
Specific heat (J/kg K)	850	850	1500	Sensible = 1800 Maximum = 5500

The hempcrete and HPCM walls were simulated for weather conditions in Ottawa, Canada. The Canadian Weather for Energy Calculations file and the modeling tool EnergyPlus were used to generate solar flux data, outside temperature, and wind speed for south wall orientation with the external heat transfer coefficient calculated by (Liu and Harris, 2015) model and the internal heat transfer coefficient estimated by (Awbi and Hatton, 1999) model.

Table 2 and Figure 2 show the simulated control techniques' implemented control logic. The base case (BC) schedule maintained setpoint temperatures between 20-24 °C, so when the temperature declined below 20 °C, heating started, and when it raised above 24 C, cooling began. Schedule 1 (SCH1) implemented heating and cooling setback temperatures of 18 °C and 26 °C, respectively, during the winter and summer dormant hours (23:00-06:00). This control method aimed to decrease heating and cooling energy consumption while facilitating the phase change transition of the microencapsulated PCM. However, our previous research revealed that hempcrete-PCM composites have a significant hysteresis effect, resulting in MPCM solidification at low temperatures (Abdellatef and Kavgic, 2020). Hence, schedule 2 (SCH2) decreased the heating setback to 16 °C while maintaining the cooling setback at 26 °C. Schedule 3 (SCH3) used 0.5 °C heating setback ramp-up and cooling setback ramp-down every 30 minutes from 05:00 to 07:00 to prevent the heating and cooling energy peaks in the morning hours. Finally, schedule 4 (SCH4) applied a 1°C heating setback temperature ramp-up every 30 minutes from 05:00 to 07:00 while maintaining the cooling controls from SCH3.

Table 2: Heating and cooling control strategy.

Mode	Heating	Cooling	Unconditioned
Active	T<20ºC	T>24ºC	20 ºC <T<24 ºC
Dormant	T<Thsb	T>Tcsb	Thsb <T< Tcsb

* Thsb and Tcsb: heating and cooling setpoint temperatures.

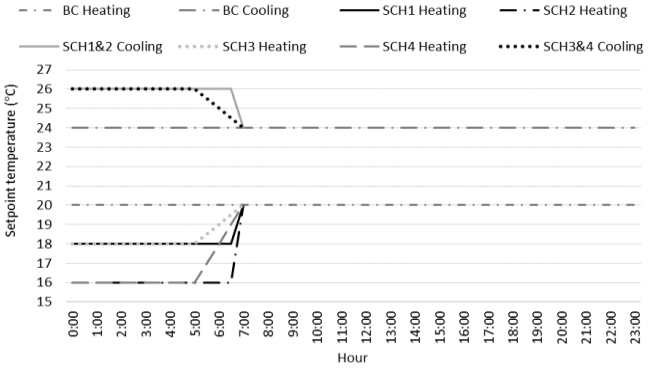

Figure 2. Heating and cooling schedules.

A finite volume method (FVM) is used to conduct the numerical analysis using ANSYS Fluent. The model solves the following time-dependent governing energy equation.

$$\rho \frac{\partial h}{\partial t} = \nabla.(k\nabla T) + S_E \quad (1)$$

where ρ is the density, t is time, h is the specific sensible enthalpy ($\int C_{p,sensible}\, dT$), k is thermal conductivity, T is temperature, and $S_{E.}$ is the source term to simulate the effect of latent energy and hysteresis, defined by the following equation (2).

$$S_E = -\rho \frac{\partial \Delta H}{\partial t} = -\frac{\rho}{\Delta t}\int_{T_{t-1}}^{T_t} (\beta(T) * L) dT \quad (2)$$

where (ΔH = βL) is the latent energy at a certain liquid fraction β, L is the total latent energy of the HPCM, T_t is the temperature at the current time step, and T_{t-1} is the temperature at the previous time step. β(T) is the liquid fraction of HPCM as a function of temperature. For the hysteresis with complete cycles of melting-freezing, the temperature change with time determines the liquid fraction equation in the source term, as shown in the following equations (3, 4).

$$S_{E,melting} = fn(\beta_m(T)), \text{ if } \frac{dT}{dt} \geq 0 \quad (3)$$

$$S_{E,freezing} = fn(\beta_f(T)), \text{ if } \frac{dT}{dt} < 0 \quad (4)$$

where $\beta_m(T)$ is the liquid fraction of the melting curve, $\beta_f(T)$ is the liquid fraction of the freezing curve. However, in real applications of PCMs into buildings' envelopes, they undergo incomplete melting and freezing conditions (Klimeš et al., 2020). Hence, a hysteresis model is used to simulate the hysteresis impact and the transition between melting and freezing curves in incomplete phase change

cycles. The hysteresis model and the liquid fraction curves are developed and validated as presented in (Kavgic and Abdellatef, 2021).

Results & discussion

Table 3 provides the annual heating, cooling, and total energy consumption with the corresponding percentage savings of the hempcrete and HPCM walls under the BC schedule. The HPCM wall reduced energy consumption compared to the hempcrete wall, with total energy savings of approximately 7.4%. The likely reason is the 10% lower thermal conductivity and improved heat storage capacity of HPCM wall than hempcrete assembly (see Table 1). Moreover, the results show that the HPCM wall achieved higher cooling than heating energy savings (21.9% cooling compared to 7.1% heating). However, due to Ottawa's cold winter heating, energy reduction was around 2184 W h/m², and cooling savings were 150 W h/m². Because these savings are per square meter, the total energy saved may be significantly higher, especially for buildings with a high volume to exposed surface ratio.

Table 3. Annual energy consumption and percentage savings under the BC schedule.

Wall Type	Consumption (Wh/m²)		Percentage Savings (%)	
	Heating	Cooling	Heating	Cooling
Hempcrete	30832	683.2	-	-
HPCM	28648	533.4	7.1	21.9

Table 4 compares the energy consumption of hempcrete and HPCM walls under control strategies SCH1 and SCH2. The implementation of setback temperatures during the night (dormant hours) in SCH1 and SCH2 decreased both walls' heating and cooling energy consumption compared to the BC. Hence, the reduction of heating setpoint by 2 °C during the dormant periods in SCH1 produced 5.3% and 5.1% heating energy reductions for hempcrete and HPCM walls, respectively, compared to the BC. Further decrease of setback temperature to 16 °C in SCH2 caused higher heating energy savings to 8.7% for hempcrete and HPCM walls. Increasing the cooling setpoint to 26 °C under both schedules caused more considerable cooling energy savings. For instance, hempcrete and HPCM walls achieved energy savings of 15.6% and 12.6%, respectively, under SCH1. Likewise, hempcrete and HPCM walls reduced cooling energy by 15.6% and 15.9%, respectively, under SCH2. Moreover, in agreement with earlier results, the HPCM wall produced higher energy savings than the hempcrete wall under SHC1 and SCH2.

Table 4. Annual energy consumption under SCH1 and SCH2.

Consumption (Wh/m²)	Schedule 1		Schedule 2	
	Hempcrete	HPCM	Hempcrete	HPCM
Heating	29207	27184	28155	26143
Cooling	576.9	466.1	576.8	448.6

Analysis of the energy consumption is required better to understand the performance of hempcrete and HPCM walls. In this regard, Figure 3 shows monthly heating and cooling energy consumption during active and dormant hours for hempcrete and HPCM walls under BC, SCH1, and SCH2. Both assemblies have higher energy consumption under SCH1 and SCH2 compared to BC during active hours. For example, the energy consumption of the hempcrete wall was 57–335 Wh/m² and 72–660 Wh/m² higher under SCH1 and SCH2, respectively, than BC. At the same time, the HPCM wall was 30–392 and 16–769 Wh/m² higher under SCH1 and SCH2, respectively, than BC. On the other hand, both SCH1 and SCH2 decreased energy consumption during dormant periods compared to the BC case throughout the year. For example, the hempcrete wall reduced energy consumption from 27% in January to 93% in July under the SCH1, whereas the HPCM wall reduced energy consumption from 31% in January to 93% in July. Moreover, the application of SCH2 further reduced energy use by 41–65% for hempcrete and 49–75% for HPCM from November to January under SCH2.

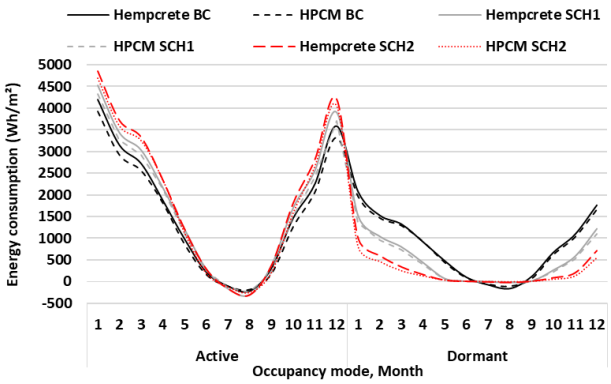

Figure 3: Average monthly heating and cooling energy consumption under BC, SCH1, and SCH2.

Figure 4 illustrates the hourly energy consumption for the three schedules (BC, SCH1, SCH2) during active and dormant hours. The most substantial increase in the heating energy consumption under SCH1 and SCH2 strategies compared to the BC case occurred in the early morning hours when the heating setback changes to the setpoint (see Figure 3). In addition, due to the more considerable

difference between setback and setpoint of 4 °C, SCH2 shows a more pronounced energy peak around 08:00 than SCH1. However, both walls achieved a significantly lower energy consumption under SCH1 and SCH2 than in the BC case at night. Furthermore, the HPCM wall outperformed the hempcrete case during dormant hours. For instance, the HPCM case had 3–6%, 5–12% and 3–32% lower hourly energy consumption than the hempcrete wall at night under BC, SCH1 and SCH2, respectively. Even though SCH1 and SCH2 saved energy relative to the base case controls, energy increases during the day and morning peaks may cause higher energy costs because of the increased energy demand during on-peak hours. As a result, we expanded our research to consider control systems that use temperature ramping to lower energy peaks in the morning and during activity hours.

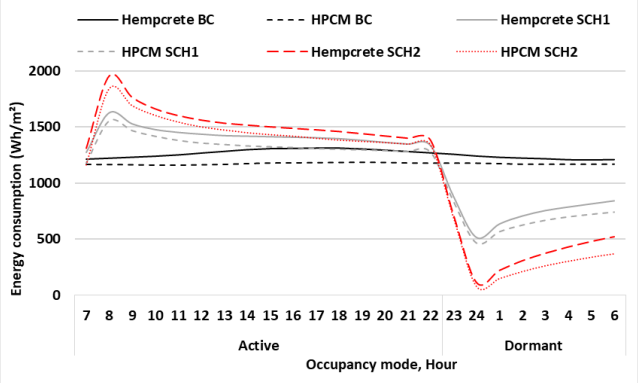

Figure 4: Average hourly heating energy consumption under BC, SCH1, and SCH2.

Table 5 presents the energy consumption of hempcrete and HPCM walls under BC, SCH3, and SCH4 schedules. Overall, implementing temperature ramping to SCH3 and SCH4 caused significant heating and cooling energy savings compared to BC and its non-ramping counterparts, SCH1 and SCH2, respectively. For instance, the heating energy reductions of SCH3 and SCH4 for both walls were approximately 13% and 25%, respectively, higher than in the BC case. The cooling energy reductions for the walls were about 66-70% higher than in the BC case. Moreover, heating energy savings in both walls were approximately 9% higher in SCH3 than in SCH1, whereas the cooling energy reductions were about 63%. In addition, the temperature ramping in SCH4 resulted in heating energy reductions of nearly 18% compared to SCH2 and the cooling energy savings of about 63% in both walls. Similar to previous results, the HPCM assembly outperformed the hempcrete wall. These findings reveal that, despite SCH3 and SCH4 having 0.2 and 0.4 °C higher average heating setback temperatures than their non-ramping counterparts, a two-hour gradual increase in setback temperatures improved the overall energy performance of the walls. The high storage capacity of hempcrete and HPCM walls is likely to explain these results because of their high specific heat capacity mixed with moderately high density.

Table 5. Annual energy consumption under BC, SCH3, and SCH4.

Consumption (Wh/m²)	Schedule 3		Schedule 4	
	Hempcrete	HPCM	Hempcrete	HPCM
Heating	26669	24843	23068	21545
Cooling	230.5	157.1	233.4	150.6

The temperature ramping in SCH3 and SCH4 significantly enhanced the hempcrete and HPCM walls' heating and cooling energy demands. Figures 5 and 6 show the monthly and hourly heating and cooling energy consumption of hempcrete and HPCM walls under SCH3 and SCH4 compared to the BC schedule. Figure 5 shows that SCH3 and SCH4 use less energy than the BC case during active and dormant seasons. For example, under SCH3 and SCH4, the walls achieved 8% to 65% and 16% to 86% higher energy savings than BC during the active heating hours. While the cooling energy savings of 73% were significantly higher than heating, the absolute numbers ranged from 76 Wh/m² to 148 Wh/m².

The results also demonstrate that SCH3 and SCH4 achieve smaller energy savings than their non-ramping peers during dormant hours compared to the BC control. As a result, both walls achieved around 6-40% and 11- 81% higher energy savings under SCH3 and SCH4, respectively, than the BC case during the nighttime. The cooling energy savings were between about 53% and 88%.

Figure 6 shows that SCH3 and SCH4 caused heating energy savings compared to the BC during most day hours. In addition, contrary to SCH1 and SCH2, the lowest hourly heating energy consumption occurred in the morning (between 7:00 and 8:00 a.m.) and early afternoon. Therefore, gradually increasing the heating setback temperatures could reduce energy prices due to the reduced demand for energy during on-peak hours.

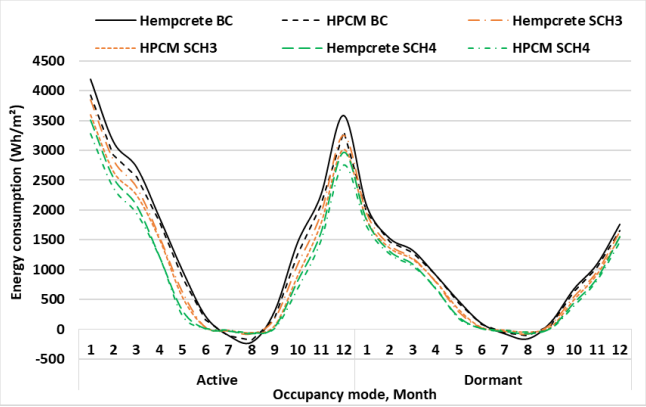

Figure 5: Average monthly heating and cooling energy consumption under BC, SCH3, and SCH4.

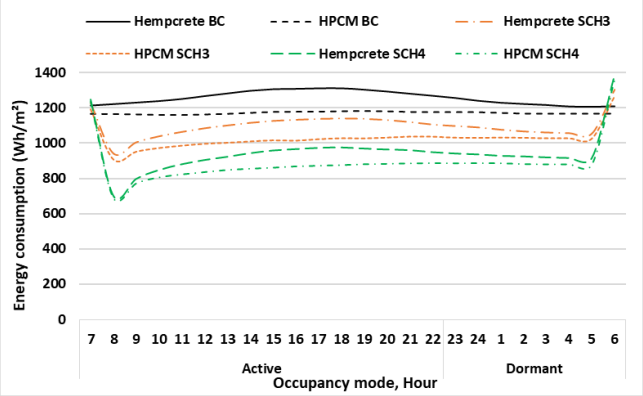

Figure 6: Average hourly heating and cooling energy consumption under BC, SCH3, and SCH4.

Figure 7 presents the performance of the HPCM wall under schedules with ramping (SCH3 and 4) and without ramping (SCH1 and 2) of the heating setpoints during the winter months from November to March. The comparison of the hourly heating energy consumption of the HPCM wall shows different performances between the four control cases. In this respect, SCH1 and SCH2 showed higher heating energy demand than SCH3 and SCH4, during active hours, by 15-35% and 28-57%, respectively. Between 08:00 and 09:00 a.m., there was a considerable change in energy demand, ranging from 29% to 57%. Conversely, SCH1 and SCH2 showed lower heating energy demand during the dormant periods than SCH3 and SCH4. The findings provide further evidence that HPCM walls can act as thermal batteries. As a result, under SCH1 and SCH2, abrupt setpoint temperature changes led the wall assemblies to charge in the morning and early afternoon, boosting energy consumption. The walls returned this heat during the night, lowering energy use. In contrast, SCH3 and SCH4 produced a lower energy demand during the day due to gradual temperature setbacks. Additionally, SCH3 and SCH4 reduced the walls' charging and discharging time during active and dormant hours.

Figure 7 also illustrates that SCH2, with a heating setback of 16 °C, had 20% to 82% higher heating energy savings during the night than SCH1, with a heating setback of 18 °C. The two control schedules had the most significant difference in heating energy consumption at midnight when the setpoint changed to the setback temperature. Nevertheless, SCH1 outperformed SCH2 by decreasing energy consumption between 11% in the afternoon and 20% in the morning. On the other hand, SCH3 and SCH4 had more consistent heating energy profiles. In this regard, SCH4 produced higher heating energy savings than SCH3 by nearly 10% at night and 10% to 20% during the daytime.

Around 06:00, one hour after the ramping period began, SCH3 performed better than SCH4. These findings agree with our previous results about the effect of the setpoint and setback temperature difference and the application time frame (Kavgic and Abdellatef, 2021). Therefore, the abrupt temperature increase over a short period in a high thermal mass material needs more energy than a gradual temperature rise over a prolonged period.

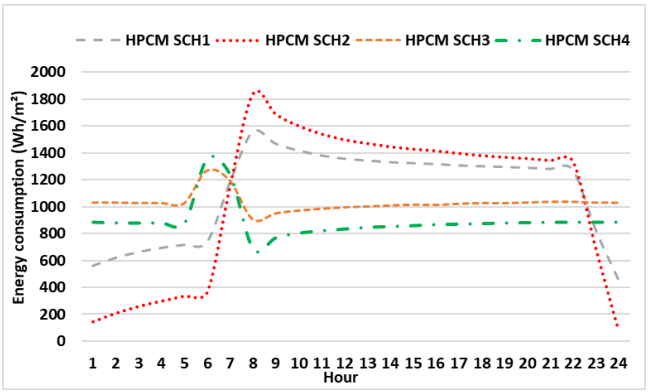

Figure 7: Average hourly heating energy consumption of HPCM10 wall under four schedules.

Table 6 presents an index to quantify the liquid fraction fluctuations ($\beta LL = (\beta max-\beta min)/(\beta max+\beta min)$) in January between Ottawa and Winnipeg (Kavgic and Abdellatef, 2021). The results show that SCH1 and SCH2 increase PCM's charging during the day and discharging during the night compared to the BC. In addition, more significant temperature fluctuation between day and night in Winnipeg increased PCM's phase transition compared to Ottawa, especially under the BC scenario. However, introducing a difference between the setpoint and setback temperatures (in SCH1 and SCH2) reduced the effect of the weather on the PCM liquid fraction fluctuations and performance.

Table 6. Liquid fraction fluctuations for Ottawa and Winnipeg.

βLL	BC	SCH1	SCH2
Ottawa	0.318	0.462	0.526
Winnipeg	0.420	0.463	0.533

Conclusion

In this research, the performance of hempcrete and HPCM walls are investigated under different control strategies to enhance the performance of latent heat storage walls in cold climates.

Under the base case schedule (BC), the HPCM wall had 7.1% and 21.9% heating and cooling energy reductions compared to the hempcrete wall, respectively. Lowering the heating setpoint to 18 °C (SCH1) and 16 °C (SCH2) during the dormant hours decreased the heating (5-9%) and cooling energy consumption (12–15%) of hempcrete and HPCM walls compared to the BC control strategy. However, SCH1 and SCH2 caused an increase in heating and cooling energy consumption in the early morning hours due to energy peaks (changing of heating setpoint from 16°C or 18°C to 20°C), which may result in higher energy costs due to the high energy demand in the on-peak hours. Moreover, increasing the difference between the active and dormant hours' heating setpoints results in higher fluctuation in PCM liquid fractions (i.e., more charging during the day and higher discharging during the night).

Modified schedules (SCH3 & 4) introduced setback temperature ramping between 05:00 and 07:00 to decrease the energy peaks in the morning and active periods. Both modified schedules result in energy savings for heating (13-25%) and cooling (65-72%). In addition, the ramping of temperature setpoint in SCH3 and SCH4 significantly improved hempcrete and HPCM walls' heating and cooling energy profiles. For example, the lowest heating energy demand was during the morning (i.e., 07:00 and 08:00) and early afternoon (compared to SCH1 & 2), which may reduce energy costs because of the lower energy demand during on-peak hours. Overall, in high thermal storage materials such as hempcrete and HPCM, the abrupt temperature increase in a short period (SCH1 & 2) requires more energy than a gradual temperature rise in an extended period (SCH3 & 4). Hence, sudden setpoint change in (SCH1 & 2) caused the walls to charge during the morning and early afternoon, increasing energy consumption. The walls discharged this energy back during the night, decreasing energy consumption. Furthermore, the gradual setback increase in (SCH3 & 4) reduced energy consumption during the daytime and reduced the heating energy savings during the dormant hours compared to (SCH1 & 2).

Future research should include sensitivity and experimental analysis to study the effect of different PCM temperatures and percentages to understand further the PCM interaction with temperature control strategies and HVAC systems. Further studies should also explore the performance and optimize the design of the HPCM walls under other Canadian climatic zones.

Acknowledgement

This research was funded by the Natural Sciences and Engineering Research Council (NSERC) Discovery Grant, grant number RGPIN-05481.

References

Environment Canada. Meteorological Service of Canada. Canadian Climate Normals. 1981-2010 Climate Normals & Averages.

Microtek Laboratories Inc. "MPCM Technical Information." https://www.microteklabs.com/.

U. S. Department of Energy. "Weather Data Sources 2019" https://energyplus.net/weather.

ABDELLATEF, Y. & KAVGIC, M. 2020. Thermal, microstructural and numerical analysis of hempcrete-microencapsulated phase change material composites. *Applied Thermal Engineering,* 178.

ABDELLATEF, Y., KAVGIC, M. & FORUZANMEHR, R. 2022. Thermal and moisture buffering properties of novel hemp-lime composites integrated with microencapsulated phase change materials. *Construction Technologies and Architecture, Trans Tech Publications Ltd.,* 1**,** 186-194.

ABDELLATEF, Y., KHAN, M. A., KHAN, A., ALAM, M. I. & KAVGIC, M. 2020. Mechanical, Thermal, and Moisture Buffering Properties of Novel Insulating Hemp-Lime Composite Building Materials. *Materials (Basel),* 13.

AL-JANABI, A. & KAVGIC, M. 2019. Application and sensitivity analysis of the phase change material hysteresis method in EnergyPlus: A case study. *Applied Thermal Engineering,* 162.

AWBI, H. B. & HATTON, A. 1999. Natural convection from heated room surfaces. *Energy and Buildings,* 30**,** 233-244.

BASTANI, A., HAGHIGHAT, F. & MANZANO, C. J. 2015. Investigating the Effect of Control Strategy on the Shift of Energy Consumption in a Building Integrated with PCM Wallboard. *Energy Procedia,* 78**,** 2280-2285.

EVRARD, A. 2008. Transient hygrothermal behavior of Lime-Hemp Materials. *PhD, Universite Catholique De Louvain.*

EVRARD, A. & HERDE, A. D. 2005. Bioclimatic envelopes made of lime and hemp concrete. *at CISBAT2005 Conference - Renewables in a Changing Climate - Innovation in Building Envelopes and Environmental Systems at Lausanne.*

FRANQUET, E., GIBOUT, S., TITTELEIN, P., ZALEWSKI, L. & DUMAS, J.-P. 2014. Experimental and theoretical analysis of a cement mortar containing microencapsulated PCM. *Applied Thermal Engineering,* 73**,** 32-40.

GHOLAMIBOZANJANI, G. & FARID, M. 2021. A Critical Review on the Control Strategies Applied to PCM-Enhanced Buildings. *Energies,* 14.

HAGENAU, M. & JRADI, M. 2020. Dynamic modeling and performance evaluation of building envelope enhanced with phase change material under Danish conditions. *Journal of Energy Storage,* 30.

KAVGIC, M. & ABDELLATEF, Y. 2021. Temperature Control to Improve Performance of Hempcrete-Phase Change Material Wall Assemblies in a Cold Climate. *Energies,* 14.

KLIMEŠ, L., CHARVÁT, P., MASTANI JOYBARI, M., ZÁLEŠÁK, M., HAGHIGHAT, F., PANCHABIKESAN, K., EL MANKIBI, M. & YUAN, Y. 2020. Computer modelling and experimental investigation of phase change hysteresis of PCMs: The state-of-the-art review. *Applied Energy,* 263.

KRASOŃ, J., MIĄSIK, P., LICHOŁAI, L., DĘBSKA, B. & STARAKIEWICZ, A. 2019. Analysis of the Thermal Characteristics of a Composite Ceramic Product Filled with Phase Change Material. *Buildings,* 9.

LECOMPTE, T., LE BIDEAU, P., GLOUANNEC, P., NORTERSHAUSER, D. & LE MASSON, S. 2015. Mechanical and thermo-physical behaviour of concretes and mortars containing phase change material. *Energy and Buildings,* 94**,** 52-60.

LIU, Y. & HARRIS, D. J. 2015. Measurements of wind speed and convective coefficient on the external surface of a low-rise building. *International Journal of Ambient Energy,* 36**,** 225-234.

NAVARRO, L., DE GRACIA, A., NIALL, D., CASTELL, A., BROWNE, M., MCCORMACK, S. J., GRIFFITHS, P. & CABEZA, L. F. 2016. Thermal energy storage in building integrated thermal systems: A review. Part 2. Integration as passive system. *Renewable Energy,* 85**,** 1334-1356.

PÉREZ-LOMBARD, L., ORTIZ, J. & POUT, C. 2008. A review on buildings energy consumption information. *Energy and Buildings,* 40**,** 394-398.

POCHWALA, S., MAKIOLA, D., ANWEILER, S. & BOHM, M. 2020. The Heat Conductivity Properties of Hemp-Lime Composite Material Used in Single-Family Buildings. *Materials (Basel),* 13.

RATHORE, P. K. S. & SHUKLA, S. K. 2019. Potential of macroencapsulated PCM for thermal energy storage in buildings: A comprehensive review. *Construction and Building Materials,* 225**,** 723-744.

REN, M., WEN, X., GAO, X. & LIU, Y. 2021. Thermal and mechanical properties of ultra-high performance concrete incorporated with microencapsulated phase change material. *Construction and Building Materials,* 273.

SOLGI, E., KARI, B. M., FAYAZ, R. & TAHERI, H. 2017. The impact of phase change materials assisted night purge ventilation on the indoor thermal conditions of office buildings in hot-arid climates. *Energy and Buildings,* 150**,** 488-497.

STANWIX, W. & SPARROW, A. 2014. The Hempcrete Book: Designing and building with hemp-lime. *Green Books, UK Hempcrete: Matlock, UK*.

TOPPI, T. & MAZZARELLA, L. 2013. Gypsum based composite materials with micro-encapsulated PCM: Experimental correlations for thermal properties estimation on the basis of the composition. *Energy and Buildings,* 57**,** 227-236.

TORRES-RODRÍGUEZ, A., MORILLÓN-GÁLVEZ, D., ALDAMA-ÁVALOS, D., HERNÁNDEZ-GÓMEZ, V. H. & GARCÍA KERDAN, I. 2020. Thermal performance evaluation of a passive building wall with CO2-filled transparent thermal insulation and paraffin-based PCM. *Solar Energy,* 205**,** 1-11.

WALKER, R. & PAVÍA, S. 2014. Moisture transfer and thermal properties of hemp–lime concretes. *Construction and Building Materials,* 64**,** 270-276.

WIJESURIYA, S., BRANDT, M. & TABARES-VELASCO, P. C. 2018. Parametric analysis of a residential building with phase change material (PCM)-enhanced drywall, precooling, and variable electric rates in a hot and dry climate. *Applied Energy,* 222**,** 497-514.

YATES, T. 2002. Final Report on the Construction of the Hemp House at Haverhill, Suffolk. *Building Research Establishment, Watford, England*.

ZHOU, D., ZHAO, C. Y. & TIAN, Y. 2012. Review on thermal energy storage with phase change materials (PCMs) in building applications. *Applied Energy,* 92**,** 593-605.

ZHU, N., WANG, S., MA, Z. & SUN, Y. 2011. Energy performance and optimal control of air-conditioned buildings with envelopes enhanced by phase change materials. *Energy Conversion and Management,* 52**,** 3197-3205.